Research Article

Rapid Communications in Mass Spectrometry

Received: 13 May 2015 Revised: 17 July 2015 Accepted: 23 July 2015 Published online in Wiley Online Library

Rapid Commun. Mass Spectrom. **2015**, *29*, 1929–1937
(wileyonlinelibrary.com) DOI: 10.1002/rcm.7288

Application of ion mobility tandem mass spectrometry to compositional and structural analysis of glycopeptides extracted from the urine of a patient diagnosed with Schindler disease

Mirela Sarbu[1,2], Feifei Zhu[3], Jasna Peter-Katalinić[4,5], David E. Clemmer[3] and Alina D. Zamfir[2,6]*

[1]West University of Timisoara, Romania
[2]Aurel Vlaicu University of Arad, Romania
[3]Department of Chemistry, Indiana University, Bloomington, USA
[4]Institute for Medical Physics and Biophysics, University of Muenster, Germany
[5]Department of Biotechnology, University of Rijeka, Croatia
[6]National Institute for Research and Development in Electrochemistry and Condensed Matter, Timisoara, Romania

RATIONALE: Schindler disease is caused by the deficient activity of α-*N*-acetylgalactosaminidase, which leads to an abnormal accumulation of *O*-glycopeptides in tissues and body fluids. In this work the Schindler condition is for the first time approached by ion mobility (IMS) tandem mass spectrometry (MS/MS), for determining urine glycopeptide fingerprints and discriminate isomeric structures.
METHODS: IMS-MS experiments were conducted on a Synapt G2s mass spectrometer operating in negative ion mode. A glycopeptide mixture extracted from the urine of a patient suffering from Schindler disease was dissolved in methanol and infused into the mass spectrometer by electrospray ionization using a syringe-pump system. MS/MS was performed by collision-induced dissociation (CID) at low energies, after mobility separation in the transfer cell. Data acquisition and processing were performed using MassLynx and Waters Driftscope software.
RESULTS: IMS-MS data indicated that the attachment of one or two amino acids to the carbohydrate backbone has a minimal influence on the molecule conformation, which limits the discrimination of the free oligosaccharides from the glycosylated amino acids and dipeptides. The structural analysis by CID MS/MS in combination with IMS-MS of species exhibiting the same *m/z* but different configurations demonstrated for the first time the presence of positional isomers for some of the Schindler disease biomarker candidates.
CONCLUSIONS: The IMS-MS and CID MS/MS platform was for the first time optimized and applied to Schindler disease glycourinome. By this approach the separation and characterization of Neu5Ac positional isomers was possible. IMS CID MS/MS showed the ability to determine the type of the glycopeptide isomers from a series of possible candidates. Copyright © 2015 John Wiley & Sons, Ltd.

Schindler disease is a rare inherited autosomal recessive disorder caused by the deficient activity of α-*N*-acetyl-galactosaminidase (NAGA), a hydrolase previously known as α-galactosidase B that cleaves the terminal α-*N*-acetylgalactosaminyl moieties from glycoconjugates.[1–7] Responsible for this lysosomal storage disease (LSD) are basically the mutations in the NAGA gene.[8] Because of the gene alteration, defects in the folding or stability of the α-NAGA occur; hence its activity within the lysosome is reduced. As a consequence, the *O*-glycan and glycopeptide enzyme substrates accumulate intralysosomally.[6] Based on the mutation site, this LSD may have an infantile or an adult onset,[9,10] while its manifestation depends on the residual activity of the mutated gene. In all types of this rare inherited condition, the enzymatic defect is severe; the enzyme residual activity ranges from only 0.5% to 2% in plasma, lymphoblasts and fibroblasts, which leads to an abnormal accumulation of sialylated and asialo-glycopeptides and oligosaccharides with α-*N*-acetylgalactosaminyl residues in various tissues and body fluids.

In human urine, complex carbohydrates are catabolic products excreted either as free oligosaccharides or linked to peptides, and their structures and amounts vary under different physiological and pathological conditions. In all types of Schindler disease, the deficient NAGA causes glycopeptiduria.[11,12] The concentration of *O*-glycans in urine was estimated to be 100 times higher than in healthy controls. For this reason, screening, structural characterization and complete identification of *O*-GalNAc glycosylated amino acids and peptides extracted from patients' urine is of major diagnostic importance.

Several reports on the investigation of Schindler disease glycourinome in the case of two male siblings diagnosed with this condition using advanced mass spectrometry (MS)

* *Correspondence to:* A. D. Zamfir, Plautius Andronescu Str. 1, Timisoara, RO-300224 Romania.
E-mail: alinazamfir@yahoo.com

methods were published in recent years.[13–15] In some instances, the analysis of the glycopeptides from patient urine was also conducted in comparison with an age-matched healthy control. Out-of-plane robotized nanochip devices for automatic sample infusion by nanoelectrospray ionization (nanoESI), polymer thin microchips for ESI, on-line coupled with either hybrid quadrupole time-of-flight (QTOF) MS,[13,16] or Fourier transform ion cyclotron resonance (FTICR) MS[17,18] were optimized and applied for screening and structural analysis of glycans and glycopeptides associated with Schindler condition. Because of the complexity of the mixture, a capillary electrophoresis (CE) technique was also on-line and off-line coupled with QTOFMS for separation, followed by compositional and structural analysis of single components in various fractions from urine of Schindler disease type I patients.[19,20]

Ion mobility spectrometry (IMS) has emerged recently as one of the most proficient separation techniques, particularly suitable for highly complex mixtures. IMS provides the separation of ions based on their differential mobility through a buffer gas. In direct coupling with MS, ion mobility spectrometry yields IMS-MS, a valuable analytical system able to separate heterogeneous mixtures, resolve ions indistinguishable solely by MS, and discriminate isomers, isobars and conformers.[21,22] Moreover, structurally similar ions and ions of the same charge state can be separated. IMS-MS was also combined with tandem mass spectrometry (MS/MS) yielding a unique platform that offers mixture separation, MS detection and structural characterization of single components by fragmentation analysis using collision-induced dissociation (CID).[23] Recently, the feasibility and benefits of IMS-MS in combination with electron transfer dissociation (ETD)[24] and electron capture dissociation (ECD)[25] were also demonstrated.

In the last few years IMS-MS was successively introduced in metabolomics,[26–28] proteomics,[29–32] lipid analysis[33] and also in glycomics,[21,34–37] and in studies related to glycosylation disorders.[38,39] However, so far IMS-MS has been much less applied to the field of lysosomal storage diseases.[40]

In the present work, Schindler disease is for the first time approached by IMS-MS and MS/MS. A complex mixture of sialylated and asialo glycans and glycopeptides extracted and purified from the urine of the younger sibling (3 years of age) diagnosed with Schindler disease was screened and sequenced using IMS-MS and MS/MS by CID.

We demonstrated here that by thoroughly optimized IMS-MS it is possible to distinguish the presence of positional isomers in Schindler disease glycourinome, and structurally confirm them by CID MS/MS sequencing in the transfer cell. Given that particular isomeric forms may exhibit structures that are readily separated and discriminated based on differences occurring in three-dimensional geometries, the IMS-MS and MS/MS methodology appears relevant for determining characteristic glycopeptide fingerprints, which may have diagnostic value for LSDs in general and Schindler disease in particular.

EXPERIMENTAL

Reagents

Analytical grade methanol and deionized water were purchased from Sigma (St. Louis, MO, USA) and used without further purification.

Biological samples

In this study, a mixture of glycosylated sialylated amino acids and peptides (denoted BP2), extracted and purified from the urine of a 3-year-old male patient presenting the clinical symptoms of Schindler disease, was investigated. The complete purification steps applied to the urine of the two siblings diagnosed with this condition are published elsewhere.[41,42] Briefly, the procedure for purification and component extraction encompasses the following steps: (i) urine filtering, followed by separation by gel filtration chromatography on Biogel P2 (BIO-RAD,UK); (ii) the resulting glycopeptide mixture was desalted by overnight incubation with H^+ beads in water at 22°C followed by 10 min centrifugation; (iii) the aqueous solution of the mixture was dried in a SpeedVac concentrator (SPD 111V-230; Thermo Electron Corporation, Asheville, NC, USA) coupled to a PC 2002 Vario vacuum pump with a CVC 2000 controller (Vaccubrand, Wertheim, Germany). For the IMS-MS experiments an aliquot of sample solution with a concentration of about 2 pmol μL^{-1} (calculated for a 2500 Da average molecular mass) was used. The aliquot was obtained by diluting the dried sample in 2:3 v/v methanol/water.

Ion mobility mass spectrometry

Ion mobility mass spectrometry experiments were conducted on a Synapt G2s mass spectrometer (Waters, Manchester, UK). The sample was directly infused into the IMS-MS system at a flow rate of 1 µL/min using a syringe-pump system. All mass spectra (MS and MS/MS) were acquired in the negative ion mode, within the mass range 50–3000 *m/z*, with a scan speed of 1 u/s. The capillary potential was varied within the range 1.5–2 kV to generate an efficient ionization of the components; however, the best result was observed at a potential of 1.8 kV. The desolvation conditions were as follows: for the desolvation gas, 600 L/h was used, while the desolvation temperature was kept at 350°C. The other parameters were adjusted and/or set as follows: the cone voltage was varied within 30–60 V, the source block temperature was kept at 100°C, while low-mass (LM) and high-mass (HM) resolution parameters were set at 12 and 15, respectively. The opening of the shutter grid allowed the release of a packet of ions that passed through the quadrupole and reached the T-wave region. As the ions migrated through the drift region under an electric field, structures with different charges, masses and/or conformations were separated according to differences in their mobility through the buffer gas. To enhance the IMS separation, IMS wave velocity was set at 650 m/s, IMS wave height at 40 V and IMS gas flow at 90 L/min. The T-wave mobility cell contained nitrogen. After separation in the drift tube, the ions were orthogonally pulsed into the TOF analyzer and further detected using the microchannel plates. The TOF analyzer was operated in the V-mode with an average mass resolution of 20,000. The selected acquisition mode was the Mobility TOF Negative Resolution MS Mode and MS/MS Mode, respectively. The fragmentation by CID was performed after mobility separation in the transfer cell, using energies between 30 and 60 V in order to provide the maximum number of diagnostic fragment ions. Data acquisition and processing were performed using MassLynx (version V4.1, SCN 855) and Waters Driftscope (version V2.7). The fragment ions were assigned using the nomenclature introduced by Domon and Costello.[43]

Rapid Communications in Mass Spectrometry

RESULTS AND DISCUSSION

Mass spectrometry in direct combination with high-performance separation techniques or microfluidics has revealed in the last decade the ability to discover in Schindler disease patient urine *O*-glycosylated amino acids and *O*-glycopeptides as potential markers useful for a rapid diagnosis.[13–19]

Considering that ion mobility separates ions based not only on their charge and mass, but also on their conformation, to test the possibility to correlate glycan and glycopeptide conformation with disease state, in the present study we examined a highly complex mixture, denoted BP2, of *O*-glycosylated sialylated amino acids and peptides previously purified from urine of a patient suffering from Schindler disease.

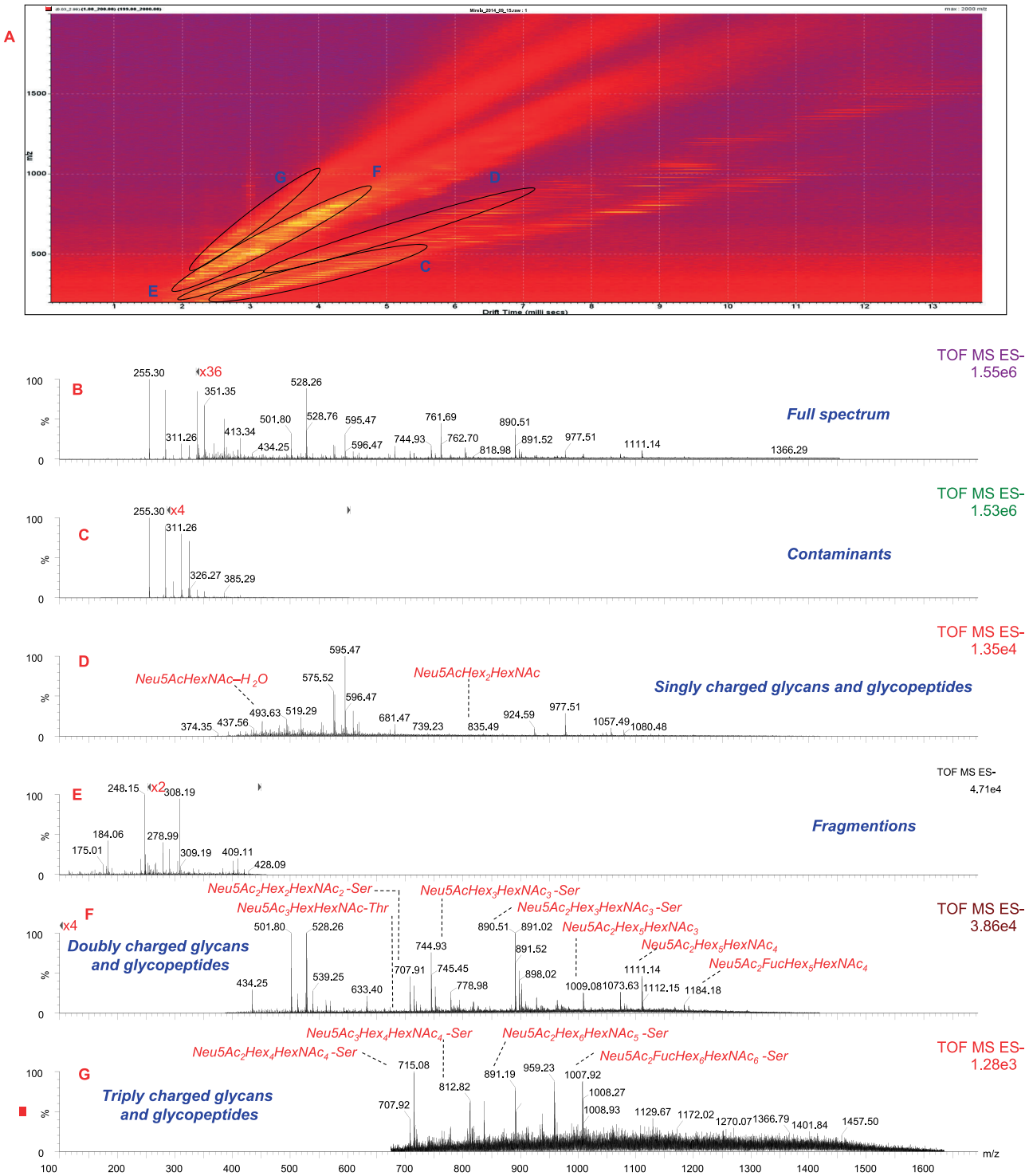

Figure 1. (A) Driftscope (*m/z*:drift time) display of the negative ions from the BP2 mixture. Circled regions correspond with the panels below. (B) Total electrospray spectrum. (C) Contaminants. (D) Singly charged glycans and glycopeptides. (E) Fragment ions. (F) Doubly charged glycans and glycopeptides. (G) Triply charged glycans and glycopeptides.

BP2 sample dissolved in 2:3 v/v methanol/water was submitted to negative ion mode ESI by syringe pump infusion. By employing ESI IMS-MS, the mobility distributions and mass spectra associated with all ions transmitted through the source were simultaneously obtained. The IMS-MS separation reduced spectral congestion by separating components into mobility families. One outcome of this separation was the reduction of background chemical noise, which was dispersed across a wide range of drift times that could be easily recognized.

According to the IMS-MS results, we have observed that the attachment of only one or two amino acids to the carbohydrate backbone had a minimal influence on the general molecule conformation, which limited the discrimination of the free oligosaccharides existing in the mixture from the glycopeptides (Fig. 1). Another important outcome was the possibility to perform structural analysis of different molecules which present the same *m/z* ratio and have different configurations. The structural characterization achieved after ion mobility separation demonstrated the presence of different conformations for some of potential Schindler disease glycopeptide biomarkers. For each signal detected in MS, the drift time(s) were extracted. Interestingly, one of these ions, namely the ion at *m/z* 677.71, of very low intensity, exhibited two mobility features, one at 3.42 ms and the other one at 3.75 ms (Fig. 2(a)).

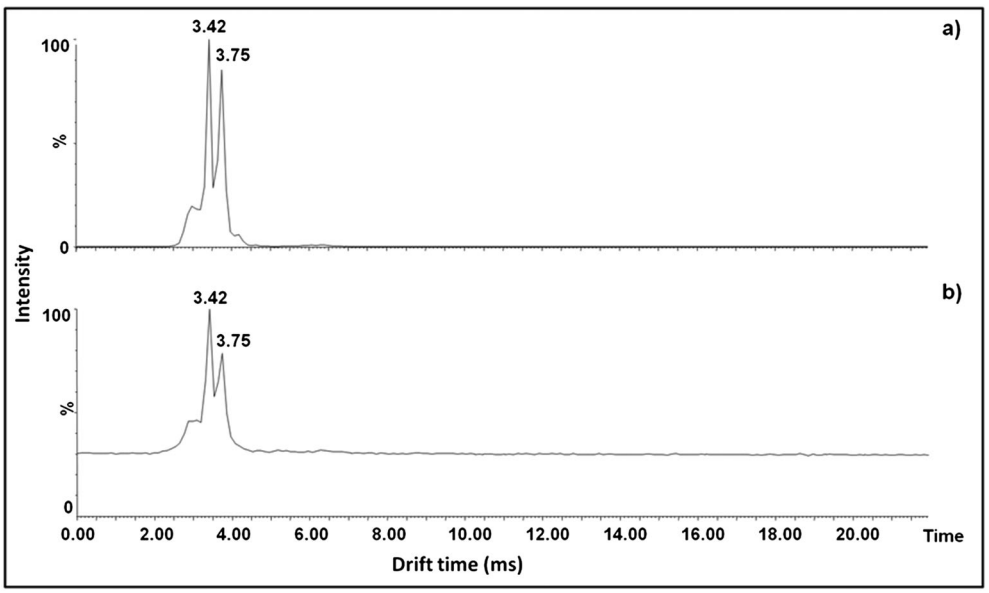

Figure 2. Drift time distribution for: (a) $[M–2H]^{2–}$ detected in MS at *m/z* 677.71 and (b) $[M–2H]^{2–}$ precursor ion at *m/z* 677.72 fragmented by CID.

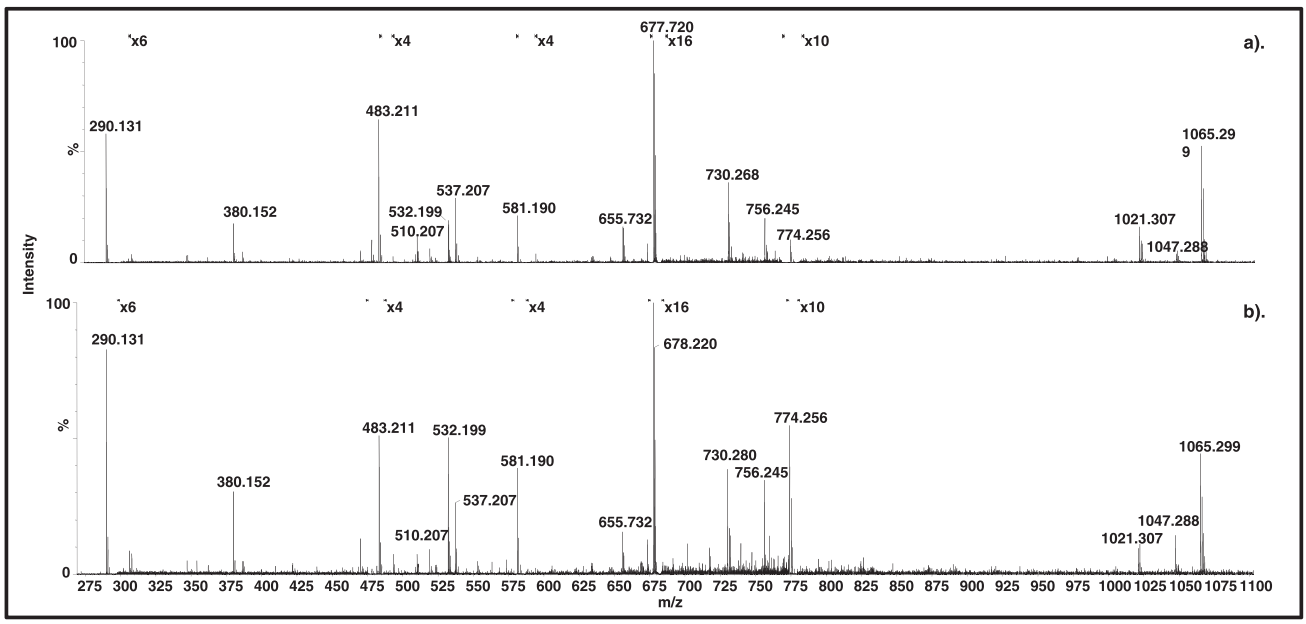

Figure 3. Extracted fragmentation spectrum of the $[M–2H]^{2–}$ precursor ion at *m/z* 677.72 from (a) the first mobility feature at 3.42 ms and (b) the second mobility feature at 3.75 ms in Fig. 2(b).

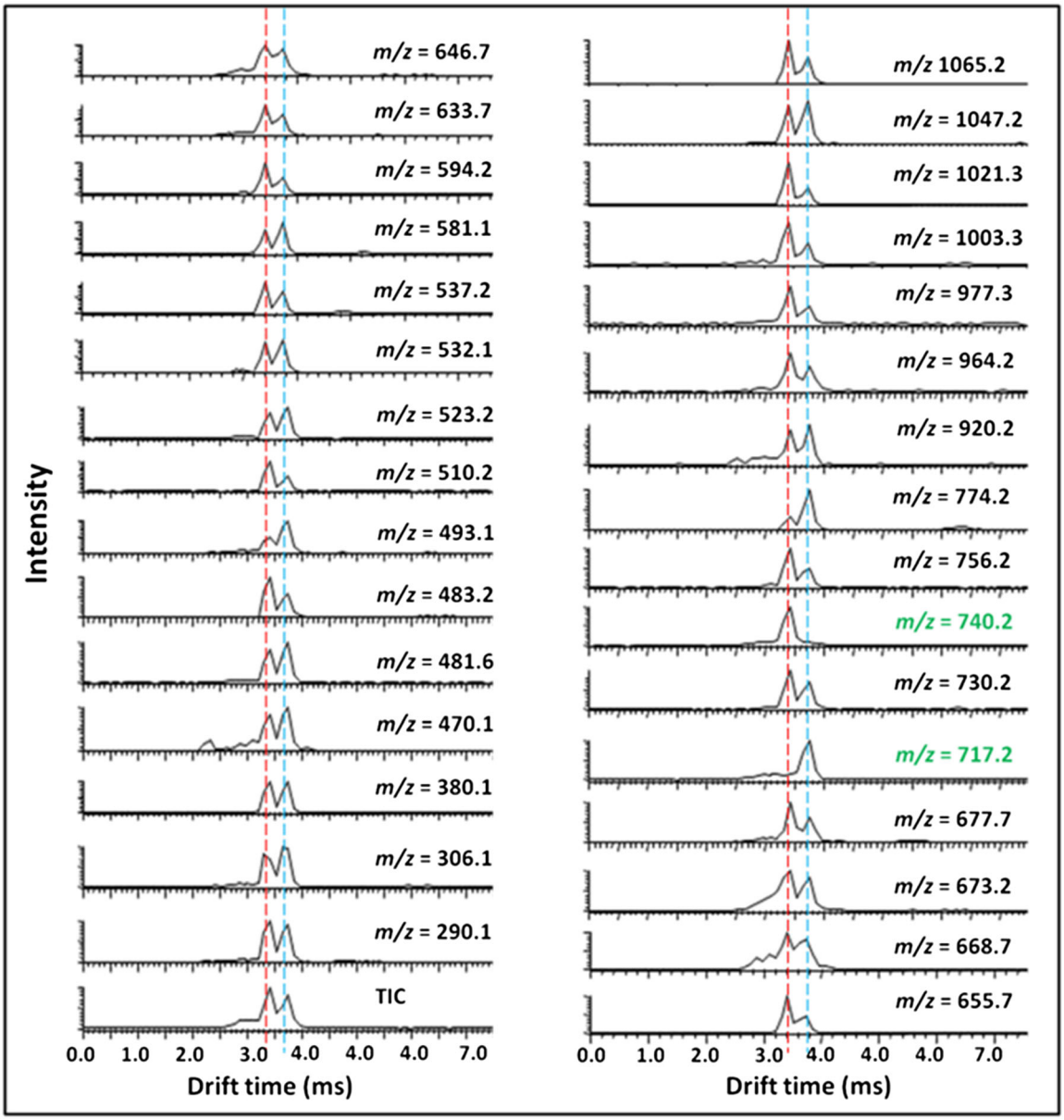

Figure 4. Drift time distribution generated by integrating over narrow regions of each fragment ion. TIC of the precursor ion fragmented by CID in the transfer cell was combined. Red line marks the t_d feature at 3.42 ms, while the blue line marks the t_d feature at 3.75 ms. The *m/z* values that exhibit only one t_d feature are shown in green.

To elucidate if the two different drift times arise from two different structures or from two isomers, the ion at *m/z* 677.71 of extremely low abundance in the spectrum in Fig. 1(F) was selected and submitted to structural characterization. The option to sequence this particular ion was also guided by the previous information collected on this substrate as follows: (i) the ion at *m/z* 677.71 was never detected in the glycopeptide mixture collected from healthy individuals, although it was found in patient urine; (ii) this species has never been structurally characterized before; (iii) it is known that in the case of complex mixtures extracted from human matrices minor species may have an important biological relevance. Fragmentation by CID using collision energies within the 30–60 eV range was performed in the transfer cell. After fragmentation, in the generated drift time distribution, the

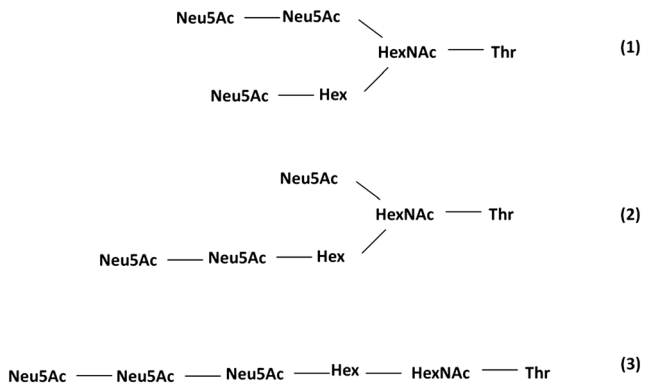

Scheme 1. Possible candidates for the molecular formula $Neu5Ac_3HexHexNAc$-Thr.

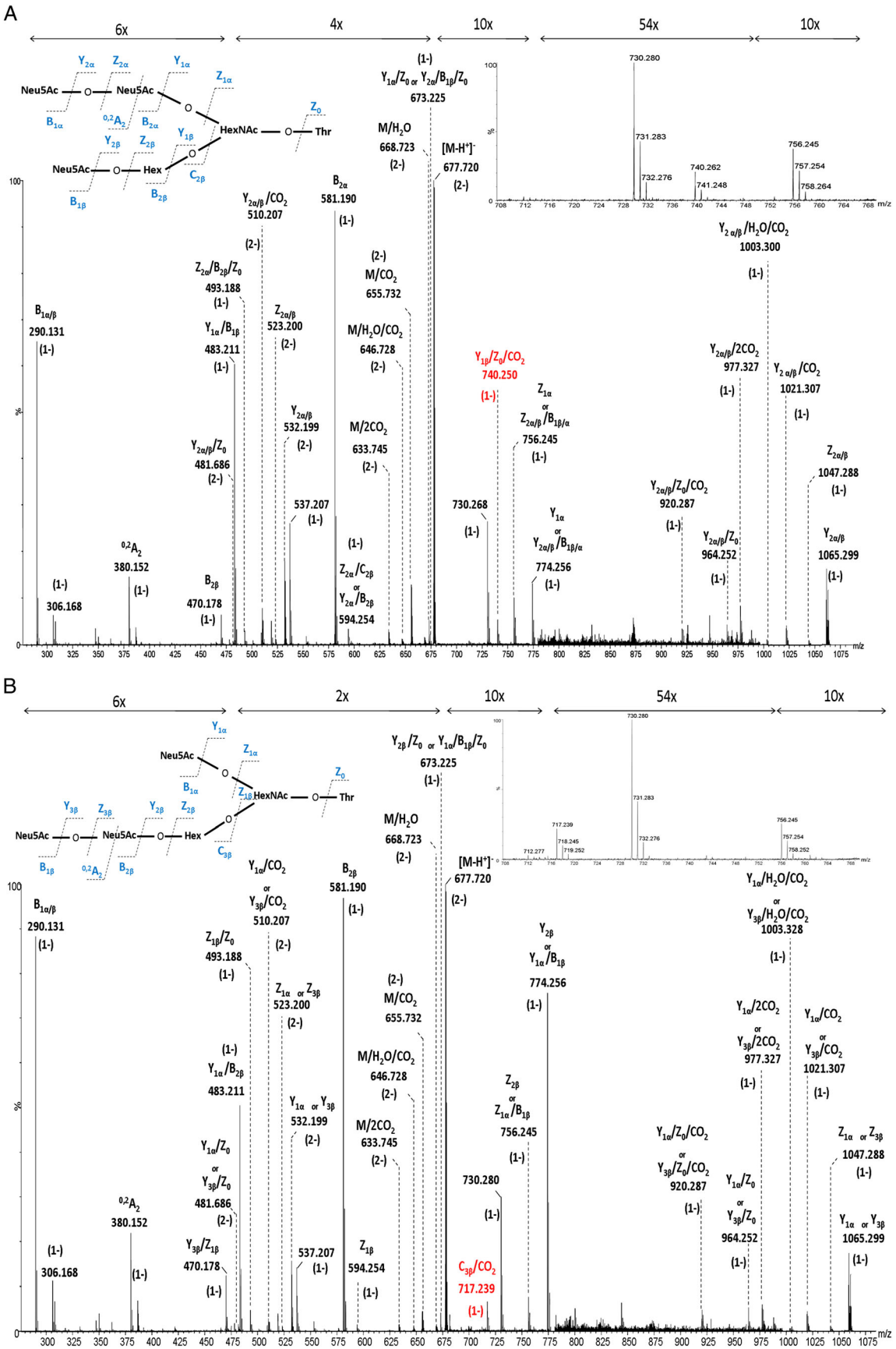

Figure 5. Fragmentation spectrum of Neu5Ac$_3$HexHexNAc-Thr precursor ion identified at *m/z* 677.720 and extracted from (a) the first mobility feature at 3.42 ms and (b) the second mobility feature at 3.75 ms of Fig. 2.

Rapid Communications in Mass Spectrometry

two mobility features could be observed again (Fig. 2(b)). The mass spectra extracted from the two mobility features are presented in Figs. 3(a) and 3(b), while in Fig. 4 the drift time distribution for all of the fragment ions generated by integrating over narrow regions of each fragment ions of the combined TIC is presented. From Figs. 3(a), 3(b) and 4, it is obvious that almost all fragment ions were characterized by two mobility features, even if they showed variability in the associated signal intensities. Exceptions are the fragment ions detected at *m/z* 717.239 and 740.250, which were found characterized by only one mobility feature. Based on these observations, the first conclusion that can be drawn is that the two mobility features observed in the MS spectra originate from different conformations of the same structure and not from two different structures. The molecular weight of 1357.48 Da corresponds to $Neu5Ac_3HexHexNAc$-Thr structure. This glycoform was already discovered in the urine of both siblings and correlated to Schindler disease in previous studies conducted using other MS approaches[42,44] but never structurally characterized by MS/MS. Hypothetically, three possible structural candidates for this molecular formula exist, as presented in Scheme 1.

The detailed interpretation of the spectra derived from the two mobility features at 3.42 ms and 3.75 ms provided evidence on a series of diagnostic fragment ions for the molecular structure. Thus, both spectra present the singly charged fragment ions at *m/z* 290.131 corresponding to Neu5Ac and at *m/z* 581.190 attributable to the disialo ($Neu5Ac_2$) element, which together with their counterparts at *m/z* 532.199 and 1065.299 as doubly and singly charged fragment ions, and at *m/z* 774.256 as the singly charged ion, confirm the sialylation of the molecule. The attachment of a Hex unit at Neu5Ac is supported in both spectra from Fig. 5 by the fragment ion detected at *m/z* 470.178. Another fragment ion, having the composition HexHexNAc-Thr, generated after the detachment of all three Neu5Ac residues, was detected at *m/z* 483.211 in both spectra. A specific product ion that is always detected in the fragmentation spectra of this type of substrates is the one at *m/z* 673.225 corresponding to Neu5AcHexHexNAc trisaccharide. A series of sequence ions generated after several neutral losses from the precursor ion are also observed in the two spectra presented in Figs. 5(a) and 5(b). This is the case of the doubly charged fragment ions at *m/z* 668.723, 655.732, 646.728 and 633.745 generated after the loss of H_2O and CO_2 and identified as M/H_2O, M/CO_2, $M/H_2O/CO_2$ and $M/2CO_2$, respectively. Other series of product ions that could be distinguished in both spectra were generated from the monodesialylated fragment ion, either by the neutral loss of CO_2 and H_2O, or by the detachment of the Thr. These series encompass: (i) the singly and doubly deprotonated fragment ions at *m/z* 481.686 and 964.252 respectively, resulting after Thr detachment; (ii) the ions at *m/z* 510.207 and 1021.307 formed after neutral loss of CO_2; and (iii) the low intensity ion at *m/z* 920.287 generated by the neutral loss of both Thr and CO_2.

The fragment ion corresponding to Neu5AcHexNAc-Thr was also observed at *m/z* 594.254. The subsequent neutral loss of Thr yielded the fragment ion at *m/z* 493.188. These two fragment ions might arise only from the first two candidates depicted in Scheme 1; the ion related to the Neu5AcHexNAc disaccharide motif could not be formed in the case of the third candidate. Consequently, the possible structural candidates that were further taken into consideration were candidate (1) and candidate (2) in Scheme 1. So far, the ions identified in the spectra support both candidates. As we mentioned before, there are only two fragment ions able to differentiate the two candidate species: the fragment ions at *m/z* 717.239 and 740.250. Except for the common ions described above, in the spectrum in Fig. 5(a), generated from the mobility feature at 3.42 ms, a signal of fair intensity was detected at *m/z* 740.250. This particular fragment ion was not found in Fig. 5(b), generated by the mobility feature at 3.75 ms. According to mass calculation, this ion corresponds to the $Neu5Ac_2HexNAc/CO_2$ structure, a fragment that documents exclusively the first candidate in Scheme 1. Therefore, this particular fragment ion, identified in Fig. 5(a) as $Y_{1\beta}/Z_0/CO_2$, strongly supports the structural configuration of the candidate (1). In contrast, in Fig. 5(b) a signal at *m/z* 717.239 was evidenced. This particular ion was, however, not detected in Fig. 5(a). According to mass calculation, the ion at *m/z* 717.239, assigned to $C_{3\beta}/CO_2$, corresponds to $Neu5Ac_2Hex/CO_2$, a sequence possible only in the case of the second candidate presented in Scheme 1. Hence, these findings corroborate candidate (2) in Scheme 1.

CONCLUSIONS

In this study a superior bioanalytical platform based on electrospray ionization ion mobility mass spectrometry in combination with collision-induced dissociation was for the first time optimized in the negative ion mode and applied to structural analysis of a glycopeptide mixture extracted and purified from the urine of a patient with Schindler disease.

By IMS-MS it was for the first time demonstrated here that the *O*-GalNAc glycosylated amino acid and peptide components in the urine of patients showing the clinical symptoms of Schindler disease present isomeric forms. Hence, Neu5Ac positional isomers were detected, separated and characterized on the basis of the mobility features, i.e. the drift time separation of sialylated glycoforms. Moreover, ion mobility separation following glycopeptide precursor ion sequencing by collision-induced dissociation in the transfer cell was able to provide the nature and detailed structure of the isomers from a series of possible candidates. Sialic acids, in particular Neu5Ac, are known to exhibit a labile linkage to the main carbohydrate core. These sugar residues readily cleave-off under most CID conditions. However, by employing negative ion mode, under appropriate sequencing conditions in terms of collision energy, gas pressure and acquisition time, an efficient fragmentation of the sialylated glycopeptide was obtained. The optimized CID parameters impeded to a reasonable extent the molecule desialylation and favored the formation of diagnostic ions for discriminating Neu5Ac positional isomers.

An interesting aspect, with biological significance, is that the $Neu5Ac_3HexHexNAc$-Thr species investigated here by IMS-MS/MS was previously identified in the urine of the same patient by studies conducted on direct- and reverse-polarity on-line CE/(–) nanoESI QTOF MS.[42,44] On the other hand, the investigations carried out by FTICRMS did not reveal the presence of $Neu5Ac_3HexHexNAc$-Thr in either of the two patients.[14,17,18] Thus, in the case of these complex mixtures, the separation prior to MS analysis appears to play

a crucial role in detection of low abundance species. The present findings are of particular significance since by IMS-MS the occurence of Neu5Ac$_3$HexHexNAc-Thr in Schindler disease could be confirmed and substantiated. Since this structure was previously not detected in the urine of the two investigated age-matched healthy individuals,[13,14] we might postulate that Neu5Ac$_3$HexHexNAc-Thr represents an important biomarker candidate for Schindler disease.

Another outcome of this study is related to the Neu5Ac$_3$HexHexNAc-Ser species which, though identified in the urine of the same patient by CE/QTOFMS,[42,44] was not detected by IMS-MS. Unlike Neu5Ac$_3$HexHexNAc-Thr, in the previous studies conducted using CE/(–)nanoESI-QTOFMS, the serine-linked homologous species was detected only in its sodiated form, as a very low intensity ion. This might explain in part the difficulty to detect it by IMS-MS. This species also presents a biological relevance for Schindler disease since it appears solely related to the patient urine; Neu5Ac$_3$HexHexNAc-Ser was never detected in the urine of the investigated healthy control.

In this context, the present findings related to the occurrence of Neu5Ac$_3$HexHexNAc-Thr positional isomers associated to the disease offer a new perspective on Schindler condition glycourinome and enlarge the inventory of potential biomarkers which can be considered for early disease diagnosis.

As Schindler disease is an extremely rare disorder, these results are based on a single case. However, the species postulated here as associated with this disease were discovered previously also by other MS methods. The present data, generated by one of the most advanced MS techniques available nowadays, provide hard evidence to support their status as disease-associated species. Certainly, other patients are to be investigated and other biochemical and biophysical methods are to be applied for the determination of the complete glycopeptide biomarker inventory in the urine of the Schindler disease patients.

Acknowledgements

MS gratefully acknowledges the fellowship provided by the strategic grant POSDRU/159/1.5/S/137750, co-financed by the European Social Fund. This work was supported by the Romanian National Authority for Scientific Research, UEFISCDI, projects PN-II-ID-PCE-2011-3-0047, PN-II-PCCA-2011-142, PN-II-PCCA-2013-4-0191 granted to ADZ and co-financed by the E.U. through European Regional Development Funds, POSCCE, through contract 621/2014.

REFERENCES

[1] D. Schindler, D. F. Bishop, D. E. Wolfe, A. M. Wang, H. Egge, R. U. Lemieux, R. J. Desnick. Neuroaxonal dystrophy due to lysosomal α-*N*-acetylgalactosaminidase deficiency. *N. Engl. J. Med.* **1989**, *320*, 1735.

[2] D. Schindler, T. Kanzaki, R. J. Desnick. A method for the rapid detection of urinary glycopeptides in α-*N*-acetylgalactosaminidase deficiency and other lysosomal storage diseases. *Clin. Chim. Acta* **1990**, *190*, 81.

[3] O. P. van Diggelen, D. Schindler, R. Willemsen, M. Boer, W. J. Kleijer, J. G. M. Huijmans, W. Blom, H. Galjaard. α-*N*-acetylgalactosaminidase deficiency, a new lysosomal storage disorder. *J. Inherit. Metab. Dis.* **1988**, *11*, 349.

[4] R. J. Desnick, A. M. Wang. Schindler disease: An inherited neuroaxonal dystrophy due to α-*N*-acetylgalactosaminidase deficiency. *J. Inherit. Metab. Dis.* **1990**, *13*, 549.

[5] R. J. Desnick, D. Schindler, in *The Molecular and Genetic Basis of Neurologic and Psychiatric Disease*, (4th edn.), (Eds: R. N. Rosenberg, S. DiMauro, H. L. Paulson, L. Ptacek, E. J. Nestler). Lippincott, Williams & Wilkins, Philadelphia, PA, **2008**, pp. 309–316.

[6] N. E. Clark, S. C. Garman. The 1.9 Å structure of human α-*N*-acetylgalactosaminidase: The molecular basis of Schindler and Kanzaki diseases. *J. Mol. Biol.* **2009**, *393*, 435.

[7] H. Sakuraba, F. Matsuzawa, S. Aikawa, H. Doi, M. Kotani, H. Nakada, T. Fukushige, T. Kanzaki. Structural and immunocytochemical studies on α-*N*-acetylgalactosaminidase deficiency (Schindler/Kanzaki disease). *J. Hum. Genet.* **2004**, *49*, 1.

[8] T. Kanekura, H. Sakuraba, F. Matsuzawa, S. Aikawa, H. Doi, Y. Hirabayashi, N. Yoshii, T. Fukushige, T. Kanzaki. Three dimensional structural studies of α-*N*-acetylgalactosaminidase (α-NAGA) in α-NAGA deficiency (Kanzaki disease): different gene mutations cause peculiar structural changes in α-NAGAs resulting in different substrate specificities and clinical phenotypes. *J. Dermatol. Sci.* **2005**, *37*, 15.

[9] K. Kodama, H. Kobayashi, R. Abe, A. Ohkawara, N. Yoshii, S. Yotsumoto, T. Fukushige, Y. Nagatsuka, Y. Hirabayashi, T. Kanzaki. A new case of alpha-*N*-acetylgalactosaminidase deficiency with angiokeratoma corporis diffusum, with Ménière's syndrome and without mental retardation. *Br. J. Dermatol.* **2001**, *144*, 363.

[10] T. Kanzaki. Schindler disease/Kanzaki disease. *Nihon Rinsho.* **1995**, *53*, 2982.

[11] T. Kanzaki, A. M. Wang, R. J. Desnick. Lysosomal alpha-*N*-acetylgalactosaminidase deficiency, the enzymatic defect in angiokeratoma corporis diffusum with glycopeptiduria. *J. Clin. Invest.* **1991**, *88*, 707.

[12] A. M. Wang, T. Kanzaki, R. J. Desnick. The molecular lesion in the alpha-*N*-acetylgalactosaminidase gene that causes angiokeratoma corporis diffusum with glycopeptiduria. *J. Clin. Invest.* **1994**, *94*, 839.

[13] A. D. Zamfir, N. Lion, Z. Vukelic, L. Bindila, J. Rossier, H. H. Girault, J. Peter-Katalinić. Thin chip microsprayer system coupled to quadrupole time-of-flight mass spectrometer for glycoconjugate analysis. *Lab Chip* **2005**, *5*, 298.

[14] L. Bindila, M. Froesch, N. Lion, Z. Vukelić, J. S. Rossier, H. H. Girault, J. Peter-Katalinić, A. D. Zamfir. A thin chip microsprayer system coupled to Fourier transform ion cyclotron resonance mass spectrometry for glycopeptide screening. *Rapid Commun. Mass Spectrom.* **2004**, *18*, 2913.

[15] M. Sarbu, A. Robu, J. Peter-Katalinić, A. D. Zamfir. Automated chip nanoelectrospray mass spectrometry for glycourinomics in Schindler disease type I. *Carbohydr. Res.* **2014**, *398C*, 90.

[16] A. Zamfir, S. Vakhrushev, A. Sterling, H. J. Niebel, M. Allen, J. Peter-Katalinić. Fully automated chip-based mass spectrometry for complex carbohydrate system analysis. *Anal. Chem.* **2004**, *76*, 2046.

[17] M. Froesch, L. Bindila, A. Zamfir, J. Peter-Katalinić. Sialylation analysis of O-glycosylated sialylated peptides from urine of patients suffering from Schindler's disease by Fourier transform ion cyclotron resonance mass spectrometry and sustained off-resonance irradiation collision-induced dissociation. *Rapid Commun. Mass Spectrom.* **2003**, *17*, 2822.

[18] M. Froesch, L. M. Bindila, G. Baykut, M. Allen, J. Peter-Katalinić, A. D. Zamfir. Coupling of fully automated chip electrospray to Fourier transform ion cyclotron resonance mass spectrometry for high-performance glycoscreening and sequencing. *Rapid Commun. Mass Spectrom.* **2004**, *18*, 3084.

[19] L. Bindila, R. Almeida, A. Sterling, M. Allen, J. Peter-Katalinić, A. D. Zamfir. Off-line capillary electrophoresis/fully automated nanoelectrospray chip quadrupole time-of-flight mass spectrometry and tandem mass spectrometry for glycoconjugate analysis. *J. Mass Spectrom.* **2004**, *39*, 1190.
[20] A. Zamfir, J. Peter-Katalinić. Capillary electrophoresis-mass spectrometry for glycoscreening in biomedical research. *Electrophoresis* **2004**, *25*, 1949.
[21] H. Li, K. Giles, B. Bendiak, K. Kaplan, W. F. Siems, H. H. Hill Jr. Resolving structural isomers of monosaccharide methyl glycosides using drift tube and traveling wave ion mobility mass spectrometry. *Anal. Chem.* **2012**, *84*, 3231.
[22] F. Lanucara, S. W. Holman, C. J. Gray, C. E. Eyers. The power of ion mobility-mass spectrometry for structural characterization and the study of conformational dynamics. *Nat. Chem.* **2014**, *6*, 281.
[23] D. J. Harvey, C. A. Scarff, M. Edgeworth, M. Crispin, C. N. Scanlan, F. Sobott, S. Allman, K. Baruah, L. Pritchard, J. H. Scrivens. Travelling wave ion mobility and negative ion fragmentation for the structural determination of N-linked glycans. *Electrophoresis* **2013**, *34*, 2368.
[24] P. Massonnet, G. Upert, N. Smargiasso, N. Gilles, L. Quinton, E. De Pauw. Combined use of ion mobility and collision-induced dissociation to investigate the opening of disulfide bridges by electron-transfer dissociation in peptides bearing two disulfide bonds. *Anal. Chem.* **2015**, *87*, 5240.
[25] A. J. Creese, A. W. Jones, D. H. Russell, H. J. Cooper. Probing the electron capture dissociation mass spectrometry of phosphopeptides with traveling wave ion mobility spectrometry and molecular dynamics simulations. *J. Am. Soc. Mass Spectrom.* **2015**, *26*, 1004.
[26] P. Dwivedi, A. J. Schultz, H. H. Hill Jr. Metabolic profiling of human blood by high-resolution ion mobility mass spectrometry (IM-MS). *Int. J. Mass Spectrom.* **2010**, *298*, 78.
[27] K. Kaplan, P. Dwivedi, S. Davidson, Q. Yang, P. Tso, W. Siems, H. H. Hill Jr. Monitoring dynamic changes in lymph metabolome of fasting and fed rats by electrospray ionization-ion mobility mass spectrometry (ESI-IMMS). *Anal. Chem.* **2009**, *81*, 7944.
[28] K. A. Kaplan, V. M. Chiu, P. A. Lukus, X. Zhang, W. F. Siems , J. O. Schenk, H. H. Hill Jr. Neuronal metabolomics by ion mobility mass spectrometry: cocaine effects on glucose and selected biogenic amine metabolites in the frontal cortex, striatum, and thalamus of the rat. *Anal. Bioanal. Chem.* **2013**, *405*, 1959.
[29] Y. Zhong, S.-J. Hyung, B. T. Ruotolo. Ion mobility–mass spectrometry for structural proteomics. *Expert Rev. Proteomics* **2012**, *9*, 47.
[30] N. F. Zinnel, P.-J. Pai, D. H. Russell. Ion mobility-mass spectrometry (IM-MS) for top-down proteomics: increased dynamic range affords increased sequence coverage. *Anal. Chem.* **2012**, *84*, 3390.
[31] P. V. Shliaha, N. J. Bond, L. Gatto, K. S. Lilley. Effects of traveling wave ion mobility separation on data independent acquisition in proteomics studies. *J. Proteome Res.* **2013**, *12*, 2323.
[32] C. Uetrecht, R. J. Rose, E. van Duijn, K. Lorenzena, A. J. R. Heck. Ion mobility mass spectrometry of proteins and protein assemblies. *Chem. Soc. Rev.* **2010**, *39*, 1633.
[33] G. Paglia, M. Kliman, E. Claude, S. Geromanos, G. Astarita. Applications of ion-mobility mass spectrometry for lipid analysis. *Anal. Bioanal. Chem.* **2015**, *407*, 4995.
[34] D. Isailovic, M. D. Plasencia, M. M. Gaye, S. T. Stokes, R. T. Kurulugama, V. Pungpapong, M. Zhang, Z. Kyselova, R. Goldman, Y. Mechref, M. V. Novotny, D. E. Clemmer. Delineating diseases by IMS-MS profiling of serum *N*-linked glycans. *J. Proteome Res.* **2012**, *11*, 576.
[35] Y. Seo, A. Andaya, J. A. Leary. Preparation, separation and conformational analysis of differentially sulfated heparin octasaccharide isomers using ion mobility mass spectrometry. *Anal. Chem.* **2012**, *84*, 2416.
[36] W. Gabryelski, K. L. Froese. Rapid and sensitive differentiation of anomers, linkage, and position isomers of disaccharides using high-field asymmetric waveform ion mobility spectrometry (FAIMS). *J. Am. Soc. Mass Spectrom.* **2003**, *14*, 265.
[37] T. Yamagaki, A. Sato. Peak width-mass correlation in CID MS/MS of isomeric oligosaccharides using traveling-wave ion mobility mass spectrometry. *J. Mass Spectrom.* **2009**, *44*, 1509.
[38] S. Y. Vakhrushev, J. Langridge, I. Campuzano, C. Hughes, J. Peter-Katalinić. Identification of monosialylated N-glycoforms in the CDG irinome by ion mobility tandem mass spectrometry: the potential for clinical applications. *Clin. Proteomics* **2008**, *4*, 47.
[39] S. Y. Vakhrushev, J. Langridge, I. Campuzano, C. Hughes, J. Peter-Katalinić. Ion mobility mass spectrometry analysis of human glycourinome. *Anal. Chem.* **2008**, *80*, 2506.
[40] M. F. Snel, M. Fuller. High-spatial resolution matrix-assisted laser desorption ionization imaging analysis of glucosylceramide in spleen sections from a mouse model of Gaucher disease. *Anal. Chem.* **2010**, *82*, 3664.
[41] J. Peter-Katalinic´, K. Williger, H. Egge, B. Green, F.-G. Hanisch, D. Schindler. The application of electrospray mass spectrometry for structural studies on a tetrasaccharide monopeptide from the urine of a patient with α-N-acetylhexosaminidase deficiency. *J. Carbohydr. Chem.* **1994**, *13*, 447.
[42] A. Zamfir, J. Peter-Katalinić. Glycoscreening by on-line sheathless capillary electrophoresis/electrospray ionization-quadrupole time of flight-tandem mass spectrometry. *Electrophoresis* **2001**, *22*, 2448.
[43] B. Domon, C. E. Costello. A systematic nomenclature for carbohydrate fragmentations in FAB-MS/MS spectra of glycoconjugates. *Glycoconjugate J.* **1988**, *5*, 397.
[44] L. Bindila, J. Peter-Katalinić, A. Zamfir. Sheathless reverse-polarity capillary electrophoresis-electrospray-mass spectrometry for analysis of underivatized glycoconjugates. *Electroporesis* **2005**, *26*, 1488.

